Upconversion emissions in Er^{3+} and Er^{3+}/Yb^{3+} activated Y_2O_3 nanopowders prepared by polymerization method

YUANXUE CAI, CHENGGUO MING*, MANTING PEI, XIAOBIN REN, ZHENGYANG YU, YUETING QIN, LIQUN AN

Department of Physics, School of Science, Tianjin University of Science & Technology, Tianjin 300457, China

Using polymerization method, Er^{3+}-doped and Er^{3+}/Yb^{3+}-codoped Y_2O_3 nanopowders were prepared. Under 975 nm excitation, upconversion emissions of the samples had been studied in detail. Strong green upconversion emission was observed in the 0.5 mol%Er^{3+}-doped Y_2O_3 nanopowder. Strong green and red upconversion emissions were discovered in the 0.5 mol%Er^{3+}/1mol%Yb^{3+}-codoped Y_2O_3 nanopowder. However, strong red upconversion emission was found in the 0.5 mol%Er^{3+}/ 5mol%Yb^{3+}-codoped Y_2O_3 nanopowder. The preparation method of luminescent nanopowders will be helpful to developing luminescent technology.

(Received August 14, 2016; accepted October 10, 2017)

Keywords: Nanopowders, Luminescence, Er^{3+}-doped

1. Introduction

Luminescent nanomaterials have been widely studied and applied to many domains, like as luminescence labeling, luminous powder, temperature sensor, and optical code [1-7], and so on. Because of the abundant energy levels of rare earth ions in the visible light region, luminous materials doped with rare earth ions have attracted people's attention [8-15]. It is known to us all, the luminous characters of rare earth ions depend on dopant concentration and crystal field environment. Trivalence Er^{3+} ion in many hosts can emit strong green emissions under near infrared excitation, which come from the transitions of Er^{3+} ion: $^2H_{11/2}/^4S_{3/2} \rightarrow {}^4I_{15/2}$ [16-18]. The preparation methods of luminous materials have high-temperature calcination, sol-gel, coprecipitation, and burning [19-22], and so on. Every method has its own merits and demerits. The nanopowder prepared by high-temperature calcination is ease, but the uniformity of the nanopowder is poor. The uniformity of the nanopowder prepared by sol-gel method is very good, but the prepared technology is complex. In this paper, we attempt to explore a new method to prepare luminous nanomaterials. And the luminescence characters of the materials have been studied in detail.

2. Experimental

Y_2O_3 nanopowders single-doped with 0.5mol% Er^{3+}, co-doped with 0.5mol% Er^{3+} and x(x=1, 5)mol% Yb^{3+} ions were synthesized by polymerization method，and marked as Er_1, $ErYb_1$, and ErYb2, respectively. The preparation procedure is described as follows: $Y(NO_3)_3 \cdot 6H_2O$, $Er(NO_3)_3 \cdot 5H_2O$, and $Yb(NO_3)_3 \cdot 5H_2O$ with corresponding mole ratios were completely dissolved in the alcoholic solution. Subsequently, methyl methacrylate was added into the solution with a mole ratio of Y to methyl methacrylate of 1:4. The solution was rapidly stirred with a magnetic stirrer at 300 K for 1h. Benzoperoxide was added into the solution, and then the solution was put into a water bath at 365K for about ten minutes. The solution was put into a drying cabinet at 320K for 48h, when it was relatively viscous like as glycerin. Until the sample becomes a transparent bulk solid, it was calcined in a high-temperature furnace at 950 K for 2 h. Finally, the sample completely turned into white powder.

X-ray diffraction (XRD) were obtained by a Bruker AXSB8 Discover model using CuK_α radiation (λ=0.154 nm). Before measuring, the samples were ground into fine powder, and the scan rate of 0.05^o min^{-1} was used to record a pattern in the 2θ range of $15\text{-}65^o$. The transmission electron micrograph (TEM) images were taken with a JEOL 4010 microscope on powder samples deposited onto a copper micro-grid coated with holey carbon. The accelerating voltage was 400 kV. The photoluminescence spectra were measured with a model F111AI fluorescence spectrophotometer. The excitation source was 975 nm laser diode (LD). The incident optical power desity is about 675 $mWcm^{-2}$, and the size of the illuminated spot is about 0.26 cm^2. The photoluminescence spectra were measured with a model F111AI fluorescence spectrophotometer. The spectral resolution of all spectra is 0.5 nm. The spectral resolution of spectrometer is 0.1 nm. The visible light was detected by photomultiplier tube detector (ZOLIX, PMTH-S1-R928). Its wavelength response range is 195-900 nm, and the sensitive wavelength is at 300-700 nm. All measurements were taken at room temperature.

3. Results and discussion

To investigate the structure of the Er_1, $ErYb_1$ and $ErYb_2$ samples, we measured the XRD of the samples. The XRD patterns of the samples were recorded and compared with the JCPDS file No83-0927, seen in Fig. 1. The spectral shape and peak intensity of the Er_1, $ErYb_1$ and $ErYb_2$ samples are the same. The sharp peaks should come from the diffraction of Y_2O_3 nanocrystal. The (h k l) values are labeled in the Fig. 1. From the measured XRD pattern peak width, the size of the nanocrystals can be calculated using the Scherer formula: $d_{hkl}=k\lambda/\beta cos\theta$, where d_{hkl} is the crystal size in the vertical direction of (hkl), β is the full width half maximum (FWHM) of the diffraction peak, θ is the angle of diffraction, λ is the wavelength of X-ray radiation (0.154 nm), and K is a constant (0.9). The average crystal sizes of Er_1, $ErYb_1$ and $ErYb_2$ samples had been calculated. The value of the average crystal size is about 45 nm, which consists with the result of TEM, seen in Fig. 2.

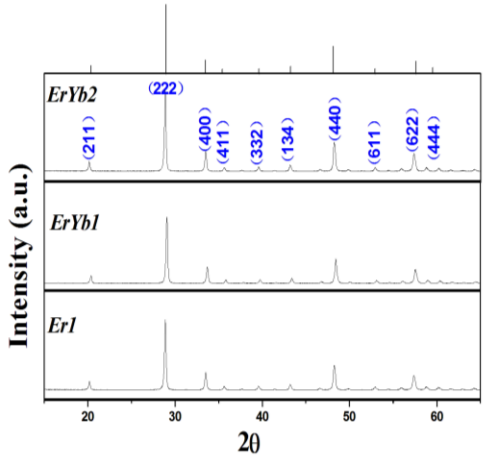

Fig. 1. XRD pattern of the Er_1, $ErYb_1$ and $ErYb_2$ samples

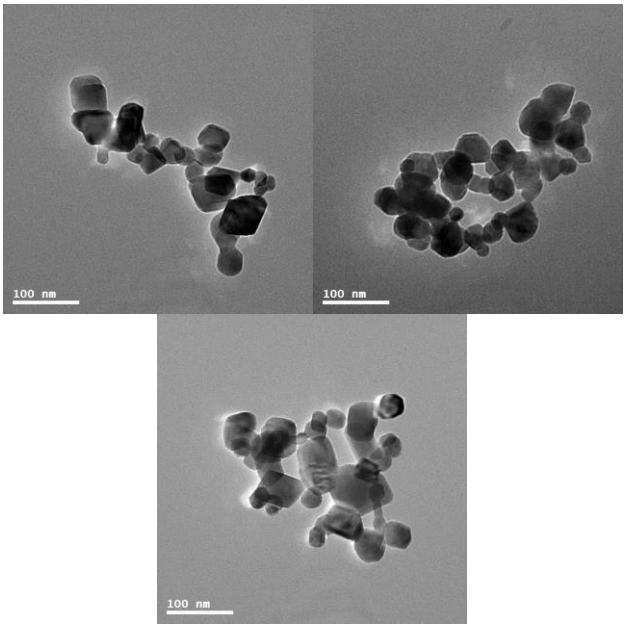

Fig. 2. TEM pattern of the Er_1, $ErYb_1$ and $ErYb_2$ samples, (a)- Er_1, (b)-$ErYb_1$, (c)-$ErYb_2$

Under 975 nm excitation, upconversion emissions of Er_1, $ErYb_1$, and $ErYb_2$ samples in the 500-750nm wavelength region are shown in Fig. 3. The strong green upconversion emission at ~560 nm is observed in the Er1 sample. The strong green and red upconversion emissions at ~560 nm and ~660nm were discovered in the $ErYb_1$ sample. However, the strong red upconversion emission at ~660nm was found in the $ErYb_2$ sample. The green emissions should come from the transition of Er^{3+} ion: $^2H_{11/2}/^4S_{3/2}\rightarrow{}^4I_{15/2}$. The red emission should be attributed to the transition of Er^{3+} ion: $^4F_{9/2}\rightarrow{}^4I_{15/2}$. The integral intensity ratio of the green upconversion emissions to the whole visible light in the Er_1 sample is 97.5%, which shows quality single-color green light. The integral intensity ratio of the red upconversion emission to the whole visible light in the $ErYb_2$ sample is 98.2%, which displays quality single-color red light.

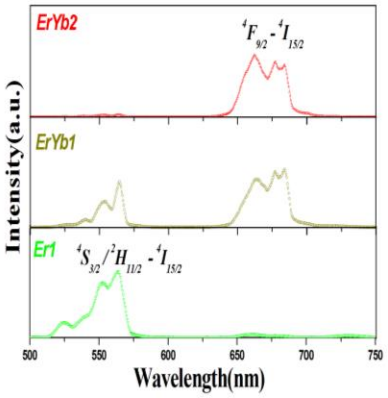

Fig. 3. Upconversion emissions of Er_1, $ErYb_1$, and $ErYb_2$ samples in the 500-750nm wavelength region under 975 nm excitation

The log-log plots for the dependence of the green and red emission integral intensities on pump power are shown in Fig. 4. According to the formula [23]: $I_{up}\propto P^n$, where I_{up} is the upconversion emission intensity, P is the pump laser power, and n represents the number of laser photons absorbed when emitting an upconversion photon. The n values of the green and red emissions in Er_1, $ErYb_1$, and $ErYb_2$ samples are indicated in Fig. 4.

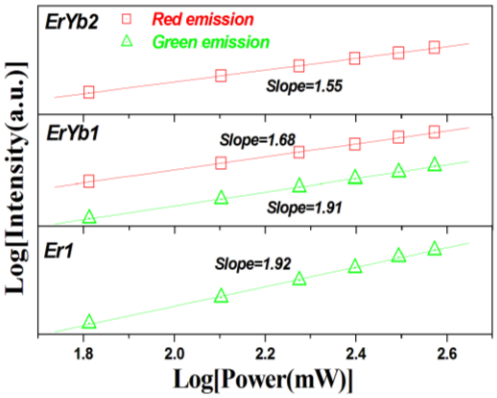

Fig. 4. Log-log plots for the dependence of the green and red emission integral intensities on pump power

The log-log plots for the dependence of the green and red emission integral intensities on pump power are shown in Fig. 4. According to the formula [23]: $I_{up} \propto P^n$, where I_{up} is the upconversion emission intensity, P is the pump laser power, and n represents the number of laser photons absorbed when emitting an upconversion photon. The n values of the green and red emissions in Er_1, $ErYb_1$, and $ErYb_2$ samples are indicated in Fig. 4.

Fig. 5 is the energy level diagrams of Er^{3+} and Yb^{3+}, as well as potential energy transition processes under 975 nm excitation. For Er^{3+}-doped Y_2O_3 nanopowder, the population processes of the green upconversion emissions can be described as follows. Er^{3+} ion in the ground state $^4I_{15/2}$ can be excited to the excited state $^4I_{11/2}$ by ground state absorption: $^4I_{15/2}(Er^{3+})+h\nu(975\,nm)\rightarrow{}^4I_{11/2}(Er^{3+})$; then, the Er^{3+} ion in the $^4I_{11/2}$ state can be pumped to the excited state $^4F_{7/2}$ by excited state absorption: $^4I_{11/2}(Er^{3+})+h\nu(975nm)\rightarrow{}^4F_{7/2}\,(Er^{3+})$; finally, the Er^{3+} ion in the $^4F_{7/2}$ state transfers to $^2H_{11/2}/^4S_{3/2}$ states by nonradiative transition, from where the green upconversion emissions arise. For Er^{3+}/Yb^{3+}-codoped Y_2O_3 nanopowder, the population processes of the strong red upconversion emission can be described as follows. Yb^{3+} ion in the ground state $^2F_{7/2}$ can be excited to the excited state $^2F_{5/2}$ by ground state absorption: $^2F_{7/2}\,(Yb^{3+})+h\nu(975nm)\rightarrow{}^2F_{5/2}\,(Yb^{3+})$; by two-step energy transitions: $^2F_{5/2}\,(Yb^{3+})+{}^4I_{15/2}(Er^{3+})\rightarrow{}^2F_{7/2}(Yb^{3+})+{}^4I_{11/2}(Er^{3+})$ and $^2F_{5/2}\,(Yb^{3+})+{}^4I_{11/2}(Er^{3+})\rightarrow{}^2F_{7/2}(Yb^{3+})+{}^4F_{7/2}(Er^{3+})$, the Er^{3+} ion in $^4I_{15/2}$ state is excited to $^4F_{7/2}$ state; then, Er^{3+} ion nonraditively transfers to $^2H_{11/2}/^4S_{3/2}$ states; by back energy transition: $^2H_{11/2}/^4S_{3/2}\,(Er^{3+})+{}^2F_{7/2}\,(Yb^{3+})\rightarrow{}^2F_{5/2}\,(Yb^{3+})+{}^4I_{13/2}(Er^{3+})$, the Er^{3+} ion transfers to $^4I_{13/2}$ state, and at the same time, Yb^{3+} ion in the ground state $^2F_{7/2}$ is excited to the excited state $^2F_{5/2}$; Finally, Er^{3+} ion in the $^4I_{13/2}$ state is pumped to $^4F_{9/2}$ state by energy transition: $^2F_{5/2}\,(Yb^{3+})+{}^4I_{13/2}(Er^{3+})\rightarrow{}^2F_{7/2}(Yb^{3+})+{}^4F_{9/2}(Er^{3+})$, from where the red upconversion emission arises.

To verify the upconversion population processes, we utilized the following steady-state equations:

$$E_0 N_{Er0} N_{Yb1} - R_2 N_{Er2} - E_2 N_{Er2} N_{Yb1} = 0, \quad (1)$$

$$E_2 N_{Er3} N_{Yb1} - R_4 N_{Er4} - B_w N_{Er4} N_{Yb0} = 0, \quad (2)$$

$$B_w N_{Er4} N_{Yb0} - E_1 N_{Er1} N_{Yb1} = 0, \quad (3)$$

$$E_1 N_{Er} N_{Yb1} - R_3 N_{Er3} = 0, \quad (4)$$

$$I\sigma N_{Yb0}/h\nu + B_w N_{Er4} N_{Yb0} - (E_0 N_{Er0} + E_1 N_{Er1} + E_2 N_{Er2}) N_{Yb1} - R N_{Yb1} = 0 \quad (5)$$

where N_{Yb0} and N_{Yb1} are the population densities of $^2F_{7/2}$, and $^2F_{5/2}$ states of Yb^{3+} ion; $N_{Er0}(E_0)$, $N_{Er1}(E_1,R_1)$, $N_{Er2}(E_2,R_2)$, and $N_{Er3}(E_3,R_3)$ are the population densities (ET rates from excited Yb^{3+}) of $^4I_{15/2}$, $^4I_{13/2}$, $^4I_{11/2}$, $^4F_{9/2}$, and $^4S_{3/2}$ states, respectively; I, ν, σ, and R are the laser intensity, the laser frequency, the absorption cross section of Yb^{3+} ion, and the radiation rate of $^2F_{5/2}$ state of Yb^{3+} ion. From Eqs.(1)-(8), the following equations can be obtain:

$$N_{Er3} = E_0 E_2 E_w N_0 N_{Yb0} N_{Yb1}^2 / R_2 R_3 (R_4 + E_w N_{Yb0}) \propto I^2, \quad (6)$$

$$N_{Er4} = E_0 E_2 N_0 N_{Yb1}^2 / R_2 (R_4 + E_w) N_{Yb0} \propto I^2. \quad (7)$$

These results agree well with the power spectra, where the red emission and the green emission are two-photon processes.

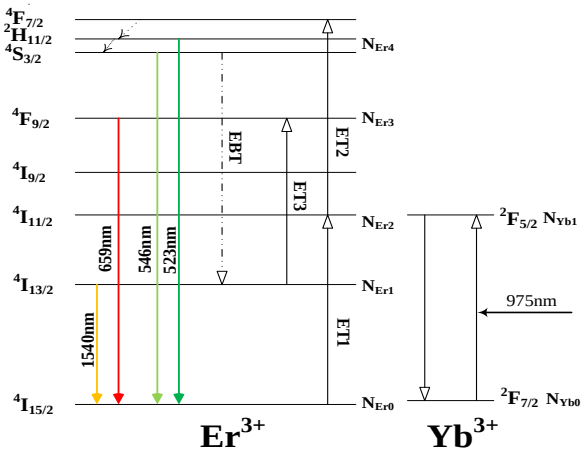

Fig. 5. Energy level diagrams of Er^{3+} and Yb^{3+}, as well as potential energy transition processes under 975 nm excitation

4. Conclusions

Using polymerization method, Y_2O_3 nanopowders single-doped with 0.5 mol% Er^{3+}, co-doped with 0.5 mol % Er^{3+} and x(x=1, 5) mol % Yb^{3+} ions were synthesized. The optical characters and luminescent mechanism of Y_2O_3 nanopowders had been discussed in detail. The strong upconversion green emissions, coming from the transitions of Er^{3+} ion: $^2H_{11/2}/^4S_{3/2}\rightarrow{}^4I_{15/2}$, were found in Y_2O_3 nanopowder single-doped with 0.5 mol% Er^{3+} ion under 975nm excitation. However, the strong red upconversion emission, being from the transition of Er^{3+} ion: $^4F_{9/2}\rightarrow{}^4I_{15/2}$, was observed in Y_2O_3 nanopowder co-doped with 0.5 mol% Er^{3+} and 5 mol % Yb^{3+} ions under 975 nm excitation. The Y_2O_3 nanopowders doped with Er^{3+} or Er^{3+}/Yb^{3+} showed good luminescent performances. Our researches will be helpful to luminescent nanotechnology.

Acknowledgments

The authors acknowledge the financial support from the National Natural Science Foundation of China under Project No. 11674183, 61405146 and 11304225, and Tianjin Research Program of Application Foundation and Advanced Technology 14CQNJC01700, And the basic research project of Tianjin higher school 2017KDYB28.

References

[1] L. Shah, Z. L. Liu, I. Hartl, G Imeshev, G C. Cho, M. E. Fermann, Opt. Express **13**(12), 4717 (2005).

[2] T. T. Huong, H. T. Phuong, H. T. Khuyen, et al., Journal of Science: Advanced Materials and Devices **1**(3), 295 (2016).

[3] S. Q. Xu, Z. M. Yang, S. X. Dai, J. H. Yang, L. L. Hu, Z. H. Jiang, J. Alloy. Compd. **361**(1-2), 313 (2003).

[4] P. A. Studenikin, A. I. Zagumennyi, Y. D. Zavartsev, P. A. Popov, I. A. Shcherbakov, Quantum. Electron. **25**(21), 1162 (1995).

[5] C. R. Li, B. Dong, S. F. Li, C. L. Song, Chem. Phys. Lett. **443**(4-6), 426 (2007).

[6] C. G Ming, F. Song, C. R. Li, Y. Yu, G Zhang, H. Yu, T. Q. Sun, J. G Tian, Opt. Lett. **36**(12), 2242 (2011).

[7] G. Y. Chen, Y. G. Zhang, G. Somesfalean, Z. G. Zhang, Appl. Phys. Lett. **89**, 16310 (2006).

[8] R. K. Tamrakar, D. P. Bisen, K. Upadhyay, et al., Superlattice. Microst. **81**, 34 (2015).

[9] R. K. Tamrakar, D. P. Bisen, K. Upadhyay, et al., J. Alloy and Compd. **655**, 423 (2016).

[10] B. Huang, Y. Zhou, F. Yang, et al., Opt. Mater. **51**, 9 (2016).

[11] H. Hu, H. Xia, P. Wang, et al., J. Nanosci. Nanotech. **16**(1), 526 (2016).

[12] C. G Ming, F. Song, L. Q. An, X. B. Ren, Appl. Phys. Lett. **102**(14), 141903 (2013).

[13] R. K. Tamrakar, D. P. Bisen, K. Upadhyay, et al., J. Phys. Chem. C **119**(36), 21072 (2015).

[14] R. K. Tamrakar, D. P. Bisen, N. Brahme, Luminescence **31**(1), 8 (2016).

[15] H. Zou, X. Wang, Y. Hu, et al., Journal of Electronic Materials **45**(6), 2745 (2016).

[16] J. C. Boyer, F. C. J. M. Van Veggel, Nanoscale **2**, 1417 (2010).

[17] H. X. Zhang, C. H. Kam, Y. Zhou, Appl. Phys. Lett. **77**(5), 609 (2000).

[18] J. F. Suyver, J. Grimm, K. W. Krämer, J. Lumin. **114**(1), 53 (2005).

[19] A. S. S. De Camargo, L. A. O. Nunes, J. F. Silva, J. Phys.: Condensed Matter **19**(24), 246209 (2007).

[20] Q. Yanmin, G Hai, J. Rare Earths **27**(3), 406 (2009).

[21] Q. Ren, R. Dai, Y. Shen, Chin. J. Lumin. **1**, 022 (2010).

[22] S. K. Singh, K. Kumar, S. B. Rai, Appl. Phys. B **94**(1), 165 (2009).

[23] F. Pandozzi, F. Vetrone, J. C. Boyer, R. Naccache, J. A. Capobianco, A. Speghini, M. Bettinelli, J. Phys. Chem. B **109**(37), 17400 (2005).

*Corresponding author: mingchengguo1978@163.com